4326 *J. Phys. Chem. A* **2004,** *108,* 4326−4334

Reactivity of Carbon-Centered Radicals toward Acrylate Double Bonds: Relative Contribution of Polar vs Enthalpy Effects

Jacques Lalevée, Xavier Allonas,* and Jean-Pierre Fouassier

Département de Photochimie Générale, UMR 7525 CNRS, Ecole Nationale Supérieure de Chimie de Mulhouse,
3 rue Alfred Werner, 68093 Mulhouse Cedex, France

Received: December 9, 2003; In Final Form: March 12, 2004

The different factors controlling the reactivity of a large series of carbon-centered radicals toward the methyl acrylate monomer unit were examined in detail by using molecular orbital calculations. In agreement with the state correlation diagram, the energy barrier is governed for a large part by the enthalpy term, as supported by an increase of reactivity with increasing exothermicity of the reaction. However, important polar effects, as evidenced by molecular calculations on the transition states, were also highlighted: they dramatically enhance the reactivity of the nucleophilic radicals (aminoalkyl or dialkylketyl radicals) as well as the electrophilic radicals (malonyl radical). Their contribution to the decrease of the barrier was evaluated by using a model based on chemical descriptors. This allows a clear separation of the relative role of the polar and enthalpy effects for 22 radicals.

Introduction

A better knowledge of the reactivity of free radicals ($R^•$) is particularly important in different fields of chemistry or biology. The radical addition to a double bond is well recognized as an appropriate way for bond-forming reaction and, for example, has long been encountered in the photoinitiation processes of radical polymerization reactions.[1] Despite its importance, radical reactivity remains the subject of large discussions, and the understanding of this basic reaction represents a fascinating challenge.[2−9] In an extensive review, experimental and theoretical works on the major factors (steric, polar, enthalpy effects) controlling the addition of carbon-centered radicals to alkenes have been recently discussed.[2] From a large set of experimental data, the role of the reaction enthalpy was empirically evaluated as an upper limiting plot of the activation energy (E_a) vs the reaction enthalpy (ΔH_r). Then, the contribution of the polar effects was taken into account by resorting to a multiplicative factor of the activation energy deduced from experimental data. The drawn conclusions and the proposed empirical model predict reasonably well the values of other addition reaction rate constants.

Despite this progress, it would be of great interest to relate the activation energy of the reaction to some physical properties of the ground-state radical or double bond. In a previous paper,[10] we found that polar effects, in addition to the usual enthalpy effects, dramatically enhance the reactivity of aminoalkyl radicals toward an acrylate monomer. To determine the structural or energetic parameters governing the addition reaction, we report here the results of molecular orbital calculations, carried out on the reactants, the products, and the transition states (TSs), for the addition of a series of carbon-centered radicals (Chart 1) to methyl acrylate (MA). These radicals possess a large variety of substituents at the radical site (having either nucleophilic or electrophilic character) so that their relative behaviors are expected to strongly change. Molecular orbital calculations on TSs will appear as a powerful tool to examine the structure−reactivity relationships in the $R^•$/MA interaction and to determine the relative contributions of both polar and enthalpy effects. A detailed analysis of the theoretical results obtained for the studied radicals as well as the use of available experimental data will help to outline, separate, and discuss the key factors controlling the radical reactivity.

CHART 1. Radicals Studied

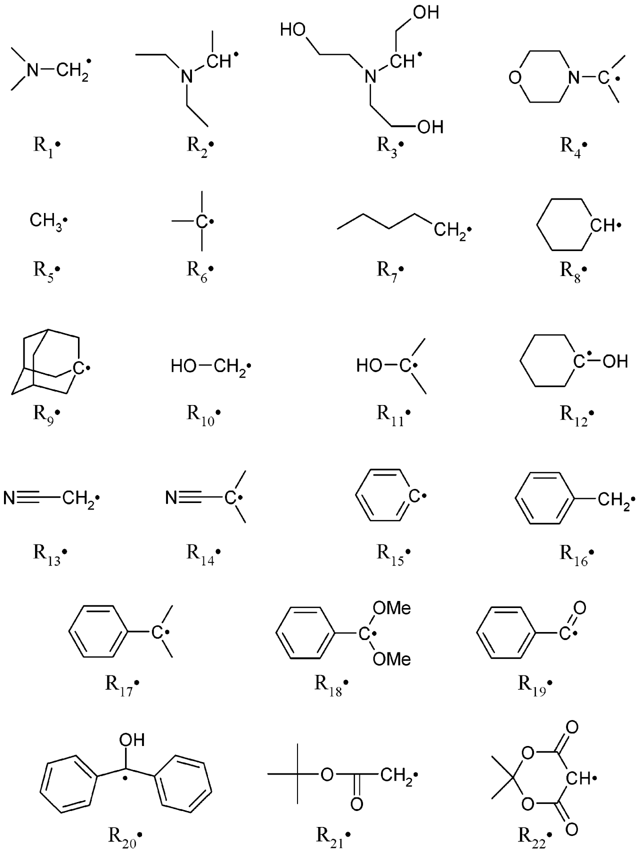

---

* To whom correspondence should be addressed. E-mail: x.allonas@uha.fr. Phone: 33 (0)389336874. Fax: 33 (0)389336895.

10.1021/jp037766g CCC: $27.50

TABLE 1: Experimental Data Characterizing the Reactivity of the Studied Radicals toward MA: Activation Energies (E_a^{exptl}) and Rate Constants of Addition (k_{obsd})

system	$E_a^{exptl\ a}$ (kJ/mol)	k_{obsd} ($M^{-1}\,s^{-1}$)	system	$E_a^{exptl\ a}$ (kJ/mol)	k_{obsd} ($M^{-1}\,s^{-1}$)
$R_2^{\bullet}$/MA		4.1×10^{7} [b]	$R_{13}^{\bullet}$/MA	18.4	1.1×10^{5} [c]
$R_3^{\bullet}$/MA		2.7×10^{7} [b]	$R_{14}^{\bullet}$/MA	29.1	370[c]
$R_4^{\bullet}$/MA		4.5×10^{7} [b]	$R_{15}^{\bullet}$/MA		1.9×10^{8} [e]
$R_5^{\bullet}$/MA	16.9	3.4×10^{5} [c]	$R_{16}^{\bullet}$/MA	33.1	430[c]
$R_6^{\bullet}$/MA	8.4	1.1×10^{6} [c]	$R_{17}^{\bullet}$/MA	26	800[f]
$R_7^{\bullet}$/MA	14.9	6.2×10^{5} [d]	$R_{18}^{\bullet}$/MA		$<1 \times 10^{4}$ [g]
$R_8^{\bullet}$/MA	10.2	3.3×10^{6} [d]	$R_{19}^{\bullet}$/MA		2.7×10^{5} [h]
$R_9^{\bullet}$/MA	1.2	1×10^{8} [d]	$R_{20}^{\bullet}$/MA		$<9 \times 10^{3}$ [i]
$R_{10}^{\bullet}$/MA	15.1	7.1×10^{5} [c]	$R_{21}^{\bullet}$/MA	15.6	4.9×10^{5} [c]
$R_{11}^{\bullet}$/MA	>0	3.5×10^{7} [c]	$R_{22}^{\bullet}$/MA	20.9	1.1×10^{5} [c]
$R_{12}^{\bullet}$/MA		2.5×10^{7} [b]			

[a] Experimental values of E_a (from refs 2 and 16). [b] From ref 10. [c] From ref 2. [d] From ref 16. [e] From ref 17. [f] From ref 15. [g] From ref 18. [h] From ref 19 for butyl acrylate. [i] From ref 20.

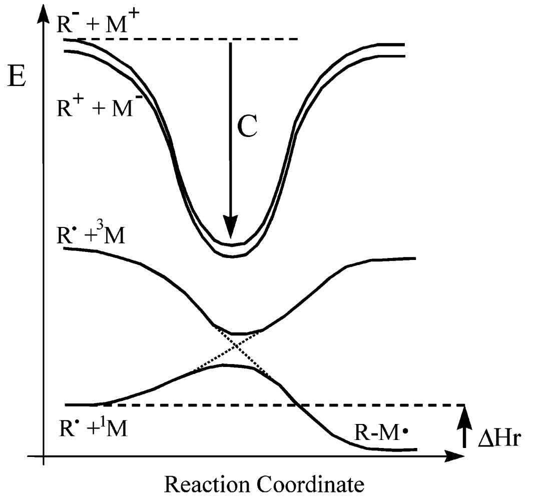

Figure 1. SCD involving the four doublet configurations of the three-center−three-electron system (C corresponds to the Coulomb interaction which stabilized the CTC). Adapted from ref 2.

Background

Experimental Data. The rate constants (k_{obsd}) for addition of the studied radicals to MA are gathered in Table 1. For the $R_2^{\bullet}$, $R_3^{\bullet}$, $R_4^{\bullet}$, and $R_{12}^{\bullet}$ radicals, k_{obsd} values have been determined previously by photoacoustic spectroscopy (PAS).[10−12] For the other radicals, rate constants are available from the literature. $R_1^{\bullet}$ is added as a model compound for comparison. k_{obsd} noticeably varies as a function of the substitution at the carbon-centered radical site: a change by 5 orders of magnitude can be observed. The values measured in the case of the aminoalkyl radicals ($R_2^{\bullet}$, $R_3^{\bullet}$, $R_4^{\bullet}$), the dialkylketyl radicals ($R_{11}^{\bullet}$, $R_{12}^{\bullet}$), the adamantyl radical ($R_9^{\bullet}$), or the phenyl radical ($R_{15}^{\bullet}$) are very high and close to the maximum values that are known for the addition of secondary or tertiary carbon-centered radicals to a double bond (10^7−10^8 $M^{-1}\,s^{-1}$).[2,13−15] For the other structures, smaller values are obtained, the extreme one being for $R_{14}^{\bullet}$ (370 $M^{-1}\,s^{-1}$).

Description of the State Correlation Diagram. A radical addition to a double bond is usually depicted by a state correlation diagram (SCD),[2,6−9] which describes the potential energy profiles of the four lowest doublet configurations of the system consisting of the unpaired electron of the radical and the electron pair of the attacked π bond (Figure 1). These configurations correspond to the reactant ground state, the reactant excited state, and two charge-transfer configurations (CTCs): R^+/M^- and R^-/M^+. From this scheme, the barrier is expected to decrease with increasing reaction exothermicity. Moreover, if the energies of the CTCs are low, their participation in the transition-state structure leads to a decrease of the barrier height.[2,8,9,13,16,21−27] Polar effects are expected to increase with decreasing energy configuration (ΔE_{CT}): $\Delta E_{CT1} = IP(R^{\bullet}) - EA(M)$ for the R^+/M^- configuration or $\Delta E_{CT2} = IP(M) - EA(R^{\bullet})$ for the R^-/M^+ one, where IP and EA stand for the ionization potential and the electron affinity of the reactants, respectively. Enthalpy and polar effects are difficult to separate, and their relative contributions remain the subject of large debates in the literature.[2,8,9,16,24,28] Nevertheless, an important participation of these CTCs is expected for ΔE_{CT} lower than 7 eV.

TABLE 2: Effect of the Level of Theory on the Computed Reaction Enthalpy (ΔH_r), Barrier Height (E_a^{TS}), and Distance between the Attacked Carbon and the Radical Center in the Transition State (d(C−C)) for the Addition Reaction of $R_5^{\bullet}$ onto MA[a]

level	$-\Delta H_r$ (kJ/mol)	E_a^{TS} (kJ/mol)	d(C−C) (Å)
B3LYP/6-311++G**//B3LYP/6-31G* [b]	106.0	21.7	2.470
B3LYP/6-31G* [b]	123.6		
B3PW91/6-311++G**//B3PW91/6-31G* [b]	119.1	20.7	2.500
B3PW91/6-31G* [b]	134.0		
B3P86/6-311++G**//B3P86/6-31G* [b]	126.7	14.8	2.528
B3P86/6-31G* [b]	141.5		
BLYP/6-311++G**//BLYP/6-31G* [b]	94.0	15.9	2.585
BLYP/6-31G* [b]	112.8		
QCISD/6-31G* [c]		34.8	2.328
QCISD/6-31G*//B3LYP/6-31G* [c]	116.1	29.2	
QCISD/6-311G**//B3LYP/6-31G* [c]	113.3	27.6	
UMP2/6-31G* [d]		63.1	2.293
UHF/6-31G* [d]	100.5	34.4	2.249
G2(MP2)[d]	110.4		
G3(MP2)-RAD[e]	107.4	21.1	
experimental[e]	111.5	17.6	

[a] Values are corrected for ZPE. [b] ZPE calculated at the corresponding DFT/6-31G* level. [c] ZPE at the B3LYP/6-31G* level. [d] With a full optimization and ZPE at this level. [e] From ref 2, reported at 0 K.

Theoretical Procedures and Results

Computational Considerations and Results. Molecular orbital calculations were performed with the Gaussian 98 suite of programs.[29] Previous studies in the literature[2,30−32] have shown that a reliable description of the barrier for chemical reaction is not straightforward. The ability of different computational methods for addition reactions to double bonds has been evaluated: high-level theoretical procedures such as UQCISD-(T), CCSD(T), CBS-RAD, or CBS-QB3 were found to give barrier values close to the experimental ones but can hardly be applied on the large molecular systems shown in Chart 1. In contrast, the B3LYP/6-311++G**//B3LYP/6-31G* procedure (i.e., single-point energy at the B3LYP/6-311++G** level performed on a fully optimized geometry at the B3LYP/6-31G* level) gave satisfactory results for several examples of addition reactions[30,33] and hence should be useful for our calculations. All these methods were compared by calculating the parameters characterizing the addition to MA (this is necessary as few calculations have been done on $R^{\bullet}$/MA): reaction enthalpy ΔH_r, activation energy E_a^{TS}, distance d(C−C) between the attacked carbon of MA and the radical center in the transition state. The experimental value and results obtained at different levels of theory are compared in Table 2 in the case of the methyl radical ($R_5^{\bullet}$).

A glance at Table 2 shows that DFT methods performed generally quite well when compared to high-level ab initio

TABLE 3: Geometrical and Energetic Parameters Computed for the Different Addition Reactions at the B3LYP/6-31G(d) Level[a]

system	$-\Delta H_r$ (kJ/mol)	d(C−C) (Å)	E_a^{TS} (kJ/mol)
$R_1^\bullet$/*c*-MA	80.1, 57^b	2.59, 2.443^c	7,^{b} 9.9^c
$R_2^\bullet$/*c*-MA	55.5, 41.1^b	2.448	2^b
$R_5^\bullet$/*c*-MA	123.3, 105.4,^{b} 106.3^c	2.474, 2.431^c	20.6,^{b} 20.7^c
$R_6^\bullet$/*c*-MA	81.5, 67.2,^{b} 67.5^c	2.387, 2.352^c	18.7,^{b} 19.4^c
$R_7^\bullet$/*c*-MA	114.7, 98^b	2.457	18.3^b
$R_{11}^\bullet$/*c*-MA	92.1, 71.5^b	2.434, 2.376^c	-2.1,^{b} −2.3^c
$R_{13}^\bullet$/*c*-MA	74.6, 61.9,^{b} 62.5^c	2.301, 2.272^c	37.2,^{b} 37.2^c
$R_{14}^\bullet$/*c*-MA	45.0, 32.4^b	2.242	44.6^b
$R_{19}^\bullet$/*c*-MA	93.5, 75^b	2.387	21.6^b
$R_1^\bullet$/*t*-MA	78.3, 54.7,^{b} 52.6^c	2.506, 2.42^c	11.7,^{b} 12.5^c
$R_2^\bullet$/*t*-MA	54, 36.7^b	2.416	10^b
$R_3^\bullet$/*t*-MA	73.8, 50.6^b	2.432	14.5^b
$R_4^\bullet$/*t*-MA	39, 21.9^b	2.364	5.1^b
$R_5^\bullet$/*t*-MA	123.6, 106,^{b} 106.3^c	2.470, 2.425^c	21.7,^{b} 21.6^c
$R_6^\bullet$/*t*-MA	78.9, 65.9,^{b} 65.7^c	2.382, 2.347^c	20.6,^{b} 20.3^c
$R_7^\bullet$/*t*-MA	113.4, 96.1^b	2.451	19.8^b
$R_8^\bullet$/*t*-MA	102.3, 85.8^b	2.432	22.5^b
$R_9^\bullet$/*t*-MA	96.2, 82.9^b	2.431	20.8^b
$R_{10}^\bullet$/*t*-MA	102.1, 87.9^b	2.477, 2.404^c	15.6,^{b} 17.1^c
$R_{11}^\bullet$/*t*-MA	82, 65.9^b	2.411, 2.358^c	7.7,^{b} 7.2^c
$R_{12}^\bullet$/*t*-MA	80.3, 61.9^b	2.38	9.2^b
$R_{13}^\bullet$/*t*-MA	75.7, 63.5^b	2.301, 2.277^c	31.3,^{b} 31.2^c
$R_{14}^\bullet$/*t*-MA	41.8, 29.4^b	2.243	50.6^b
$R_{15}^\bullet$/*t*-MA	168.1, 154.2^b	2.596	7.2^b
$R_{16}^\bullet$/*t*-MA	60.9, 46.4^b	2.265	34.9^b
$R_{17}^\bullet$/*t*-MA	27.4, 13.4^b	2.216	45.9^b
$R_{18}^\bullet$/*t*-MA	7.1, −8.6^b	2.230	56.9^b
$R_{19}^\bullet$/*t*-MA	92.4, 73.8^b	2.386	23.1^b
$R_{20}^\bullet$/*t*-MA	1.3, −13.1^b	2.104	70.9^b
$R_{21}^\bullet$/*t*-MA	91.7, 76^b	2.349	22.3^b
$R_{22}^\bullet$/*t*-MA	69.5, 53.5^b	2.273	26.2^b

[a] See the legend of Table 2. [b] B3LYP/6-311++G**//B3LYP/6-31G* (ZPE at the B3LYP/6-31G* level). [c] Full optimization at the B3LYP/6-311++G** level (ZPE included).

methods, with the great advantage of being less demanding in computational time. Despite some small differences, the results obtained with the B3LYP/6-311++G** procedure were found in very good agreement with both the results of high-level calculations (G3(MP2)-RAD) and experimental measurements. For the barrier, hybrid functionals (B3LYP and B3PW91) lead to results consistent with those of the G3(MP2)-RAD procedure. This confirms some previous remarks on the ability of these DFT methods in evaluating the activation energy.[34,35] The results obtained at this level are even better than those obtained with the QCISD/6-31G* or QCISD/6-311G** procedures, thereby demonstrating the interest of our approach. The effect of the basis set toward ΔH_r has been evaluated for these different functionals: the reaction enthalpy computed with DFT methods using the 6-31G* basis set is 15.6 kJ/mol higher than that computed with an extended basis set. From the different functionals studied in Table 2, B3LYP gave good results for the reaction enthalpy with a difference of about 10 kJ/mol. Finally, the B3LYP/6-311++G**//B3LYP/6-31G* procedure appears as very convenient to reproduce the trends observed for the barrier and will be used in the following.

Geometrical and energetic parameters computed for the different addition reactions are gathered in Table 3. Some previous computational results obtained[10] for the $R_1^\bullet - R_6^\bullet$ and $R_{11}^\bullet$ radicals have been added to extend our analysis to a large set of radical structures.

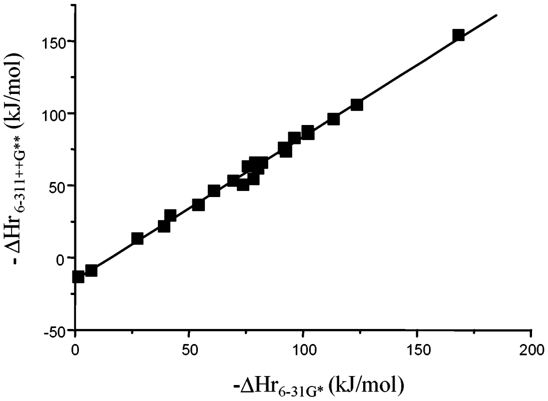

Figure 2. Effect of the level of theory on the calculated reaction enthalpies.

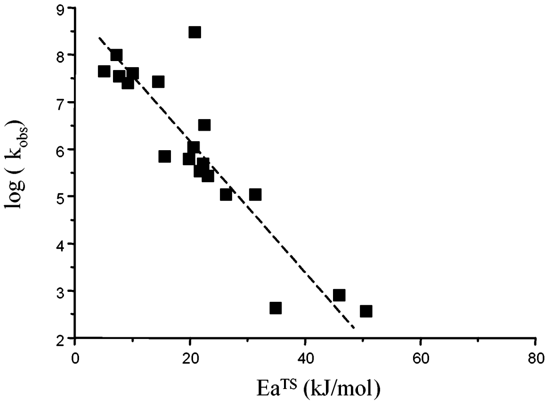

Figure 3. Observed rate constants k_{obsd} vs the computed energy barriers E_a^{TS} (B3LYP/6-311++G**//B3LYP/6-31G*).

For the systems studied, the enthalpies calculated with an extended basis set correlate fairly well (Figure 2) with those found at the 6-31G* level, leading to the following relationship:

$$\Delta H_{r,6-311++G^{**}} = 0.99\Delta H_{r,6-31G^*} + 15.6 \qquad (1)$$

The computation at the B3LYP/6-31G* level of theory being less time-consuming, we will mainly use the results obtained at this level for further discussions.

As already pointed out,[10,36] the energy difference between the *cis* and *trans* structures of MA is not significant and the two forms were assumed to coexist in solution. The transition states for the addition of different radicals ($R_1^\bullet$, $R_2^\bullet$, $R_5^\bullet$, $R_6^\bullet$, $R_7^\bullet$, $R_{11}^\bullet$, $R_{13}^\bullet$, $R_{14}^\bullet$, $R_{19}^\bullet$) to *cis*- and *trans*-methylacrylates are defined in Table 3. Since the difference in reactivity between the two isomers is, as expected, very low and the geometrical and energetic parameters are always very similar in most cases for the two structures,[37] the discussion will then be mostly restricted to the results obtained on the *trans* form.

Comparison of the Theoretical Calculations with the Experimental Data. The dependence of the addition rate constants k_{obsd} on the calculated barrier E_a^{TS} is shown in Figure 3 ($R_{18}^\bullet$ and $R_{20}^\bullet$ were withdrawn from the figure, as the corresponding rate constants are only known as upper limits). Despite the well-known difference in preexponential factors (A) on going from primary ($10^{7.5}$) to tertiary ($10^{8.5}$) radicals,[2] the quite good correlation observed gives confidence to the ability of the theoretical method used to reproduce the experimental trend. By the way, it also confirms that the preexponential factor of the Arrhenius law remains reasonably constant, as already suggested.[2] A plot of the calculated barriers (E_a^{TS}) vs the experimental ones (E_a^{exptl}) yields a slope of 0.97 and an intercept of 10.4 kJ/mol, although the data are scattered ($r^2 = 0.65$). The discrepancies observed can arise from three factors: (i) the experimental barrier values have a higher uncertainty than those of the addition rate constants, particularly when the former have been deduced from the corresponding addition rate constant for carbon-centered radicals by using an average preexponential factor,[2] (ii) an intrinsic error (±5 kJ/mol[30]) associated with the theoretical procedure used should be taken into account, (iii) the calculated values, obtained in the same way as generally in the literature, correspond to gas-phase data contrary to the experimental ones that are measured in solvents (a complete analysis of the solvent effects is beyond the scope of the present work and will be developed in a forthcoming paper). All these effects were already pointed out and were shown to restrict any attempt to relate in a simple way experimental and calculated energy barriers.[30]

Regioselectivity of the Addition Reaction onto MA. The regioselectivity of the addition reaction has been the subject of important experimental and theoretical works: the major mode of addition occurs at the less substituted carbon, the addition on the most substituted carbon being rather scarce.[7,38−40] Theoretical investigations have demonstrated that two factors play a role in this process: the spin density in the triplet state and the reaction exothermicity. We have recently shown[10] that addition to the less substituted carbon of MA is largely favorable; i.e., it leads to the most exothermic reaction and corresponds to the most spin rich carbon in the $\pi\pi^*$ triplet state. As a consequence, the barrier for the addition at this site is lower than that for the most substituted carbon (e.g., 15 kJ/mol for $R_1^{\bullet}$ and $R_5^{\bullet}$ at the B3LYP/6-31G* level). The following discussion will refer to *t*-MA.

Discussion

Influence of the Reaction Enthalpy. The plot of the activation energy E_a^{TS} as a function of the reaction enthalpy ΔH_r shows that a more favorable barrier corresponds to a higher reaction exothermicity as expected from the SCD (Figure 4). However, some data clearly depart from this general behavior, which suggests a participation of polar effects that enhance the reactivity of several radicals toward the acrylate unit. Indeed, the aminoalkyl radicals $R_1^{\bullet}$, $R_2^{\bullet}$, $R_3^{\bullet}$, and $R_4^{\bullet}$ (for which polar effects were previously demonstrated[10]) and the dialkylketyl radicals $R_{11}^{\bullet}$ and $R_{12}^{\bullet}$ are clearly out of the correlation. The exclusion of these compounds leads to a fairly good correlation (dot line in Figure 4) corresponding to

$$E_a^{TS} = 60 + 0.37\Delta H_{r,6-31G^*} \qquad (2)$$

Using the extended basis set, eq 2 turns into $E_a^{TS} = 44.3 + 0.37\Delta H_{r,6-311++G^{**}}$. Such an Evans−Polanyi relationship has already been obtained for some radical addition reactions (see below).[2]

The location of the transition-state structure in the SCD[2,7] is mainly determined by the crossing between the reactant and product configurations, while the energy of the TS structure can be influenced by the charge-transfer configurations. In the TS structures obtained, the bond formation roughly correlates with $\Delta H_{r,6-31G^*}$ (Figure 5), in agreement with Hammond's postulate, which states that the earliness of a transition structure is directly related to the reaction exothermicity. However, the points concerning the aminoalkyl radicals are still clearly beyond the correlation; i.e., the structures of the corresponding TSs are earlier than expected from their reaction enthalpies (difference of about 0.12 Å by using the correlation obtained for the other compounds). In a more general way, the TS structure is mainly controlled by the reaction enthalpy, while very strong polar effects (as observed for aminoalkyl radicals[10]) lead to the TS earlier than expected. Indeed, an important participation of the CTC to the TS structure can influence the position of the avoided crossing leading to this earlier TS. This shows that the enthalpy factor, although important, cannot alone explain the reactivity.

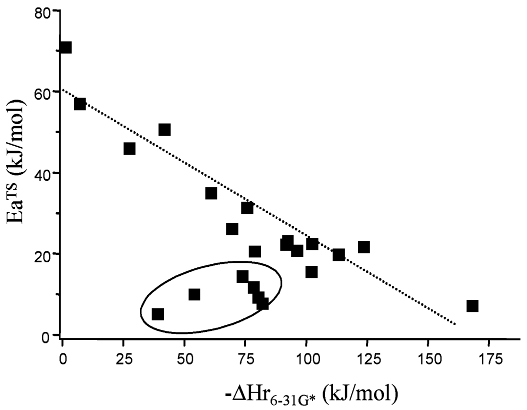

Figure 4. Reaction enthalpies $\Delta H_{r,6-31G^*}$ vs the computed barriers E_a^{TS} (points corresponding to $R_1^{\bullet}-R_4^{\bullet}$, $R_{11}^{\bullet}$, and $R_{12}^{\bullet}$ are encircled).

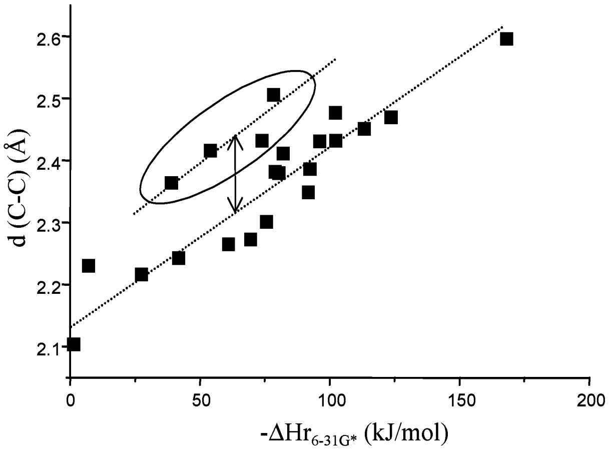

Figure 5. Evolution of d(C−C) with the enthalpy of the reaction ΔH_r (points corresponding to $R_1^{\bullet}-R_4^{\bullet}$ are encircled).

Polar Effects. *Charge-Transfer Configurations*. The IP and the EA of the different radicals studied are gathered in Table 4. Adiabatic ionization potentials were determined by DFT methods by using IP = E(cation) − E(radical) after full geometry optimization for both the radical and cation. The same procedure was applied to the calculations of EA. Calculated and experimental IP and EA values exhibit a very good agreement with differences lower than 0.4 eV. Moreover, the effect of the basis set is negligible, the differences being usually lower than 0.2 eV for IP or EA when using 6-31G* and 6-311++G** basis sets.

Using IP = 9.8 eV and EA = −0.49 eV for MA,[2] the energy of the different CTCs can be determined. As said above, the importance of the polar effects increases as the configuration energy ΔE_{CT} decreases. From the calculations reported in Table 4, radicals $R_1^{\bullet}-R_4^{\bullet}$, $R_9^{\bullet}$, $R_{11}^{\bullet}$, $R_{12}^{\bullet}$, $R_{17}^{\bullet}$, $R_{18}^{\bullet}$ and $R_{20}^{\bullet}$ present mainly a nucleophilic behavior toward MA with a low R^+/M^- charge-transfer energy ($\Delta E_{CT1} < 7$ eV): this result is ascribed to the very low IP of these radicals and to the strong electron-deficient character of MA (high EA). On the contrary, the R^-/M^+ CTC is very favorable for $R_{22}^{\bullet}$ with $\Delta E_{CT2} < 7$ eV. An even better indication of the nucleophilic/electrophilic character of the radicals toward MA is offered by the ratio $R = \Delta E_{CT1}/\Delta E_{CT2}$. The lowest R values are obtained for the aminoalkyl

TABLE 4: Energetic Parameters Characterizing the Different Charge-Transfer Configurations Involved in the Addition Reaction at the B3LYP/6-31+G(d) Level[a]

radical	IP($R^\bullet$) (eV) calcd[b]	IP($R^\bullet$) (eV) exptl	EA($R^\bullet$) (eV) calcd[b]	EA($R^\bullet$) (eV) exptl	ΔE_{CT1} (eV)	ΔE_{CT2} (eV)	R
$R_1^\bullet$	5.62, 5.66[c]	5.7[g]	−0.4, −0.31[c]		6.11	10.2	0.60
$R_2^\bullet$	4.96, 4.98[c]		−0.35		5.45	10.15	0.54
$R_3^\bullet$	5.43		0.58		5.92	9.22	0.64
$R_4^\bullet$	4.9		−0.28		5.39	10.08	0.53
$R_5^\bullet$	9.9	9.84,[d] 9.8[e]	0.00	0.08,[d] 0.1[e]	10.39	9.8	1.06
$R_6^\bullet$	6.78	6.7[e]	−0.18	−0.16,[d] 0[e]	7.27	9.98	0.73
$R_7^\bullet$	7.5	7.94[f]	−0.11		7.99	9.91	0.81
$R_8^\bullet$	7.04	7.66[f]	−0.08		7.53	9.88	0.76
$R_9^\bullet$	6.17	6.21[f]	−0.02		6.66	9.82	0.68
$R_{10}^\bullet$	7.67, 7.73[c]	7.56,[d] 7.6[e]	−0.22, −0.18[c]	0.1[e]	8.16	10.02	0.81
$R_{11}^\bullet$	6.25, 6.28[c]	6.5[e]	−0.21, −0.11[c]	0.3[e]	6.74	10.01	0.67
$R_{12}^\bullet$	6.01		−0.08		6.5	9.88	0.66
$R_{13}^\bullet$	10.29, 10.33[c]	9.9,[d] 10.3[e]	1.52, 1.58[c]	1.5[e]	10.78	8.28	1.30
$R_{14}^\bullet$	8.42, 8.42[c]	8.5[e]	1.06	1[e]	8.91	8.74	1.02
$R_{15}^\bullet$	8.25	8.32[d]	1.06		8.74	8.74	1.00
$R_{16}^\bullet$	7.15	7.24,[d] 7.2[e]	0.84	0.91,[d] 0.9[e]	7.64	8.96	0.85
$R_{17}^\bullet$	6.45	6.6[e]	0.67		6.94	9.13	0.76
$R_{18}^\bullet$	5.66		0.59		6.15	9.21	0.67
$R_{19}^\bullet$	6.58		0.69		7.07	9.11	0.78
$R_{20}^\bullet$	5.94		1.13		6.43	8.67	0.74
$R_{21}^\bullet$	8.00		1.64		8.49	8.16	1.04
$R_{22}^\bullet$	9.91, 9.85[c]		3.23, 3.28[c]		10.4	6.57	1.58

[a] See the text. [b] Adiabatic ionization potential and electron affinity at B3LYP/6-31+G(d) after optimization of the geometry of the radical and the cation or the anion (ZPE included). [c] Same method with fully optimized structures at the B3LYP/6-311++G** level. [d] From ref 41. [e] From ref 2. [f] From ref 16. [g] From ref 42.

TABLE 5: Effect of the Basis Set[a] **on the Charge-Transfer Character (δ^{TS}) for the Addition of $R_1^\bullet$ and $R_5^\bullet$ to MA**

	6-31G*	6-31+G*	6-311++G**
$R_1^\bullet$/MA	0.143	0.112	0.158, 0.134[b]
$R_5^\bullet$/MA	0.02	0.023	0.021, 0.02[b]

[a] Full optimization with the B3LYP functional. [b] Single point with the 6-311++G** basis set on the 6-31G* geometry.

radicals ($R = 0.5-0.6$) and the dialkylketyl radicals ($R = 0.67$ and 0.66 for $R_{11}^\bullet$ and $R_{12}^\bullet$, respectively), outlining their high nucleophilic character. The other radicals have a lower nucleophilic character ($R = 0.7-0.9$ for $R_6^\bullet-R_{10}^\bullet$ and $R_{16}^\bullet-R_{20}^\bullet$). The $R_5^\bullet$, $R_{14}^\bullet$, $R_{15}^\bullet$, and $R_{21}^\bullet$ radicals have no marked nucleophilic or electrophilic behavior (*R* ratio close to 1). For $R_{13}^\bullet$ and $R_{22}^\bullet$, an electrophilic behavior is expected ($R = 1.3$ and 1.58, respectively). These results indicate that a low IP can strongly enhance the reactivity owing to an important stabilization of the TS through the CTC: radicals that fulfill this requirement (e.g., aminoalkyl and dialkylketyl radicals) will present the most important polar effects and, as a consequence, depart from the E_a^{TS} vs $\Delta H_{r,6-31G*}$ correlation line (Figure 4).

Polar Effects in the Transition States. A direct evaluation of the charge-transfer (CT) character was obtained from the charge transferred from the radical to the double bond (δ^{TS}), which was calculated from the Mulliken analysis in the TS.[2,8,9,43] The effect of the basis set on δ^{TS}, examined in Table 5, is rather weak on going from the 6-31G* level to the 6-311++G** level: the results obtained at the 6-31G* level appear to be accurate enough for the description of the systems studied.

δ^{TS} values on $R^\bullet$ for the different $R^\bullet$/MA couples are shown in Table 6. As expected, the values of the systems with low CTC energies are remarkably large (0.14−0.2 for aminoalkyl or dialkylketyl radicals). From a more general point of view, an excellent correlation is observed when *R* or IP is plotted vs δ^{TS} (Figure 6). These results are of prime importance since they directly connect the properties of the isolated species (IP, EA) with the CT character in the TS and allow the evaluation of δ without any calculation of the corresponding TS.

TABLE 6: $\chi_R^\bullet$ and $\eta_R^\bullet$ Values. Parameters Characterizing the Charge Transfer in the TS[a]

system	δ^{TS} [b]	$\chi_{R\bullet}$ (eV)	$\eta_{R\bullet}$ (eV)	δ^{PP} [c]	ΔE_{pol}^{PP} [c] (kJ/mol)
$R_1^\bullet$/*t*-MA	0.143	2.61	3.01	0.125	12.4
$R_2^\bullet$/*t*-MA	0.199	2.31	2.65	0.151	17.1
$R_3^\bullet$/*t*-MA	0.174	3.00	2.425	0.11	8.7
$R_4^\bullet$/*t*-MA	0.194	2.31	2.59	0.152	17.2
$R_5^\bullet$/*t*-MA	0.02	4.95	4.95	−0.015	0.2
$R_6^\bullet$/*t*-MA	0.096	3.3	3.48	0.079	5.1
$R_7^\bullet$/*t*-MA	0.05	3.69	3.80	0.054	2.5
$R_8^\bullet$/*t*-MA	0.071	3.48	3.56	0.067	3.8
$R_9^\bullet$/*t*-MA	0.08	3.08	3.1	0.096	7.3
$R_{10}^\bullet$/*t*-MA	0.084	3.72	3.94	0.051	2.3
$R_{11}^\bullet$/*t*-MA	0.129	3.02	3.23	0.098	7.7
$R_{12}^\bullet$/*t*-MA	0.139	2.96	3.04	0.103	8.4
$R_{13}^\bullet$/*t*-MA	−0.048	5.90	4.38	−0.065	3.9
$R_{14}^\bullet$/*t*-MA	−0.001	4.74	3.68	−0.005	0.02
$R_{15}^\bullet$/*t*-MA	−0.001	4.66	3.60	0	0
$R_{16}^\bullet$/*t*-MA	0.045	4.00	3.16	0.040	1.3
$R_{17}^\bullet$/*t*-MA	0.092	3.56	2.89	0.068	3.6
$R_{18}^\bullet$/*t*-MA	0.151	3.12	2.54	0.100	7.3
$R_{19}^\bullet$/*t*-MA	0.088	3.64	2.94	0.063	3.1
$R_{20}^\bullet$/*t*-MA	0.1	3.54	2.40	0.074	4.0
$R_{21}^\bullet$/*t*-MA	−0.02	4.82	3.18	−0.010	0.1
$R_{22}^\bullet$/*t*-MA	−0.118	6.57	3.34	−0.112	10.4

[a] See the text. [b] Charge transfer obtained at the B3LYP/6-31G* level. [c] Charge transfer calculated from the Parr and Pearson model.

The influence of the CT between the two reactants on the rate constant is difficult to quantify and separate from the influence of the reaction enthalpy. To study the relative role of these factors in our case, the plot of E_a^{TS} vs $\Delta H_{r,6-31G*}$ and $|\delta^{TS}|$, represented in Figure 7, is particularly convenient. Both $\Delta H_{r,6-31G*}$ and $|\delta^{TS}|$ terms influence E_a^{TS}: for a given value of $\Delta H_{r,6-31G*}$, an important decrease of the barrier is observed with increasing δ^{TS}. In the same way, for a given value of $|\delta^{TS}|$, a more favorable reaction enthalpy decreases the barrier. The strong effects of these two factors are evidenced by different changes in the reactivity ordering that cannot be accounted for when only one factor is considered. For example, despite their

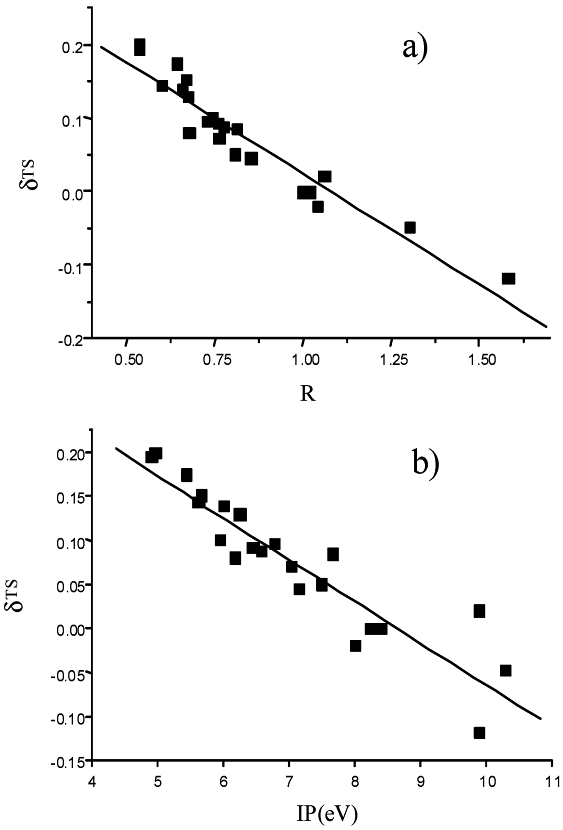

Figure 6. (a) Computed charge-transfer δ^{TS} vs the ratio R and (b) δ^{TS} vs the ionization potential of the radical.

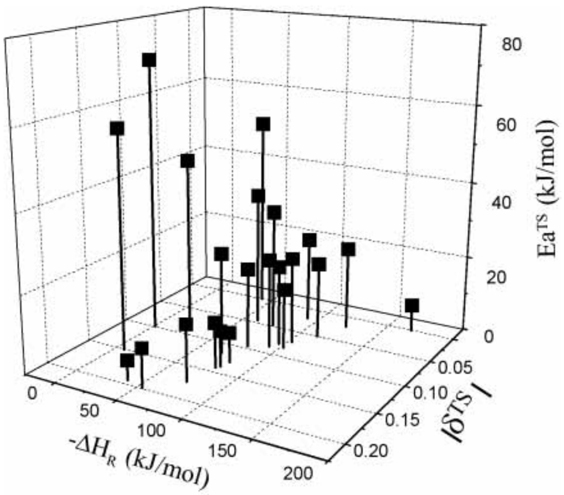

Figure 7. Evolution of the calculated barriers $E_a{}^{TS}$ with the charge-transfer characters δ^{TS} and the reaction enthalpies $\Delta H_{r,6-31G^*}$.

higher or similar $\Delta H_{r,6-31G^*}$, the $E_a{}^{TS}$ values calculated for the alkyl radicals ($R_5{}^\bullet$ and $R_9{}^\bullet$) are always higher than those found for the aminoalkyl radicals. This result is clearly in line with the large CT character observed for these compounds, thereby supporting an important decrease of the barrier through a large participation of the CTC in the TS. An opposite effect is noted when $R_{15}{}^\bullet$ is compared to the alkyl radicals: despite a value $\delta^{TS} \approx 0$, the barrier for $R_{15}{}^\bullet$ is largely lower than for $R_5{}^\bullet - R_9{}^\bullet$, in accordance with a higher reaction exothermicity.

To separate the polar and enthalpy effects, Parr and Pearson's model (PP) was used to evaluate the energy released by the charge transfer.[44−48] This method was successfully used to describe the addition reaction of peroxy radicals to alkenes.[49,50] In this PP model, the absolute electronegativity (χ) and hardness (η) of the different radicals are calculated from the IP and EA values, by the following equations:

$$\chi = (\mathrm{IP} + \mathrm{EA})/2 \tag{3}$$

$$\eta = (\mathrm{IP} - \mathrm{EA})/2 \tag{4}$$

When $R^\bullet$ and M are brought together, the electron will flow from the molecule that possesses the lower χ to that with the higher χ. According to the electronegativity equalization principle, the charge-transfer δ^{PP} can be estimated from these parameters characterizing the isolated reactants

$$\delta^{PP} = \frac{(\chi_M - \chi_{R\bullet})}{2(\eta_M + \eta_{R\bullet})} \tag{5}$$

and the polar energy change $\Delta E_{pol}{}^{PP}$, due to this charge transfer, is then expressed by

$$\Delta E_{pol}{}^{PP} = \frac{(\chi_M - \chi_{R\bullet})^2}{4(\eta_M + \eta_{R\bullet})} \tag{6}$$

In this model, the absolute electronegativity difference is the driving factor for the charge-transfer ability whereas the sum of the hardnesses inhibits it. The calculated δ^{PP} and $\Delta E_{pol}{}^{PP}$ parameters are gathered in Table 6 using 4.655 and 5.145 eV for the χ_M and η_M values of MA, respectively (calculated from experimental data).

The CT properties ($\chi_{R\bullet}$, δ^{PP}) determined from this model can be compared to the results found by molecular calculations. An excellent correlation between δ^{TS} and $\chi_{R\bullet}$ is observed in Figure 8a, in accordance with eq 5. The correlation is even better than that obtained previously between δ^{TS} and IP when $\delta^{TS} < 0$. This is a feature of the better description of the CT character of the electrophilic radicals by $\chi_{R\bullet}$ rather than by IP: indeed, the absolute electronegativity takes into account the acceptor properties of the radical by including EA in the calculations (eq 3), whereas the ionization potential describes the donor properties (this behavior is particularly evidenced in $R_{22}{}^\bullet$). Interestingly, the correlation between the charge transfer calculated by this model (δ^{PP}) and that obtained by molecular calculations (δ^{TS}) is really remarkable with a slope close to unity (Figure 8b).

According to eqs 3−6, ΔE_{pol} is directly related to δ^{PP}. Indeed, the data of Table 6 for the $R^\bullet$/MA systems are fairly well fitted with a parabola as shown in Figure 9, leading to

$$\Delta E_{pol}{}^{PP} = a(\delta^{PP})^2 \quad \text{with} \quad a = 775\ \mathrm{kJ/mol} \tag{7}$$

The PP model provides an accurate evaluation of the CT character between the reactants in the transition-state structures. This, in turn, can be used to quantitatively separate the contribution of the polar effect from that of the enthalpy on the barrier.

Separation of the Polar and Enthalpy Effects. In the following, to take into account the possible changes in the geometry of the transition state compared to reactant ground states, the polar energy change $\Delta E_{pol}{}^{PP}$ will be preferably determined by using the computed δ^{TS} values (eq 8). The

$$\Delta \mathrm{E}_{pol} = 775\ (\delta^{TS})^2 \tag{8}$$

calculation of ΔE_{pol} from δ^{TS} is expected to be more accurate because the use of IP and EA, which assumes that the reactants

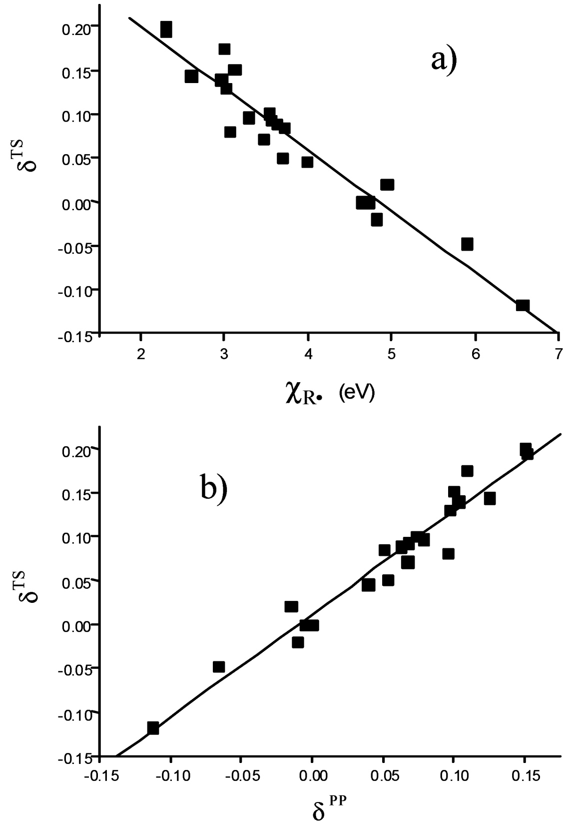

Figure 8. (a) Charge-transfer characters δ_{TS} vs the absolute electronegativities $\chi_{R\bullet}$. (b) Correlation of the calculated charge-transfer δ^{TS} in the TS with the charge-transfer δ^{PP} calculated with Parr and Pearson's model.

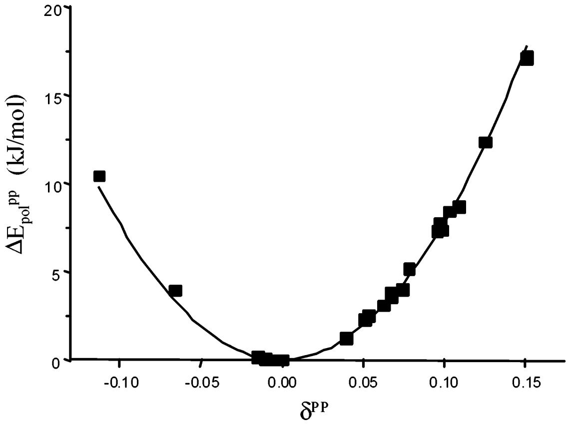

Figure 9. Polar energy change ΔE_{pol}^{PP} vs the charge-transfer δ^{PP}.

keep their identity in the TS structure, is avoided: slight modifications of IP and EA due to some molecular deformations in the TS cannot be excluded.

Deciphering the relative effect of charge transfer and enthalpy in the energy barrier is a tricky problem. Recently, a multiplicative scheme[2] has led to an empirical relationship which, for some radicals, satisfactorily accounts for the experimental results, although the theoretical basis of this scheme remains unclear. With the premise that the good agreement between δ^{TS} and δ^{PP} demonstrates that ΔE_{pol} is not dependent on the reaction enthalpy, we assumed an additivity scheme for the enthalpic and polar contributions to the energy barrier. This is a widely accepted approach[51] that presents the great advantage of being fully compatible with the Parr−Pearson calculation of the polar energy.[49,50,52] Therefore, the enthalpy term (E_{enth}) is calculated from the activation energy E_a^{TS} value and taking into account the stabilization energy ΔE_{pol} associated with the charge transfer in the TS:

TABLE 7: Separation of the Polar and Enthalpy Contributions

radical	ΔE_{enth} (kJ/mol)	ΔE_{pol} (kJ/mol)	$\Delta E_{pol}/(\Delta E_{pol} + \Delta E_{enth})$
1	31.9	15.8	0.33
2	22.0	30.7	0.58
3	30.0	23.5	0.44
4	15.9	29.2	0.65
5	50.3	0.3	0.006
6	32.1	7.1	0.18
7	46.1	1.9	0.04
8	41.6	3.9	0.09
9	39.1	5.0	0.11
10	41.5	5.5	0.12
11	33.4	12.9	0.28
12	32.7	15	0.31
13	30.8	1.8	0.06
14	17.0	0.0	0.00
15	68.4	0.0	0.00
16	24.8	1.6	0.06
17	11.1	6.5	0.37
18	2.9	17.7	0.86
19	37.6	6.0	0.14
20	0.5	7.7	0.94
21	37.3	0.3	0.01
22	28.3	10.8	0.28

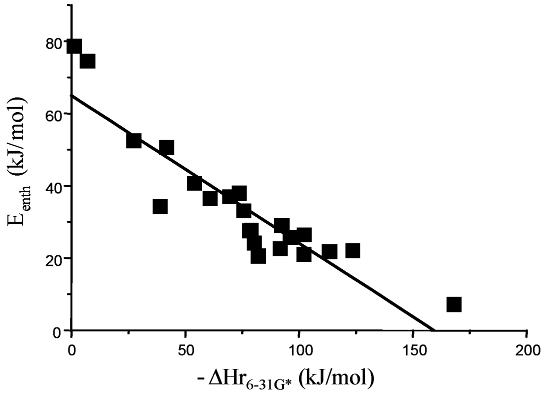

Figure 10. Enthalpy terms E_{enth} vs the reaction enthalpies $\Delta H_{r,6-31G^*}$.

$$E_a^{TS} = E_{enth} - \Delta E_{pol} \tag{9}$$

Equation 9 allows a clear separation of both the polar and enthalpy contributions. The E_{enth} values are easily deduced from the computed E_a^{TS} and the calculated ΔE_{pol} (Table 7). The plot of E_{enth} vs $\Delta H_{r,6-31G^*}$ is shown in Figure 10. A quite good linear relationship, significantly better than that observed in Figure 4, holds true (it must be recalled that the good linear relationship eq 2 was only due to the exclusion of the radicals presenting strong polar effects):

$$E_{enth} = E_a^0 - \Delta E_{enth}$$

$$E_{enth} = 64.9 + 0.41\Delta H_{r,6-31G^*} \tag{10}$$

E_a^0 is the energy barrier at $\Delta H_r = 0$ and in the absence of any polar effect, and ΔE_{enth} is the contribution of the enthalpy to the barrier height. This relationship becomes $E_{enth} = 49.2 + 0.41\Delta H_{r,6-311++G^{**}}$ when using the extended basis set. The dispersion of the points along this line can still arise from the large variety of the studied structures for which slight steric or electronic effects can be expected: this is particularly true for $R_{20}^{\bullet}$, $R_{18}^{\bullet}$ ($\Delta H_{r,6-31G*}$ close to 0 kJ/mol), and $R_{15}^{\bullet}$ ($\Delta H_{r,6-31G*} = -168.1$ kJ/mol), which correspond to the worst points in the correlation. More generally, eq 10 corresponds to an Evans−Polanyi relationship, which states that the barrier decreases increasing exothermicity. In the present case, between one-third and half of the ΔH_r change is transferred to the TS structure. A different approach has led to an empirical limit for the reaction enthalpy effect on the barrier,[2] $E_{enth} = 50 + 0.22\Delta H_{r,exptl}$, knowing that, in that case, the $\Delta H_{r,exptl}$ values have been calculated from thermodynamic cycles and gas-phase quantities, a procedure which likely leads to a more important uncertainty[2] (the differences might have an influence since a plot of $\Delta H_{r,6-31G*}$ vs $\Delta H_{r,exptl}$ shows that $\Delta H_{r,exptl} = 1.15\Delta H_{r,6-31G*} + 19.9$, with $r^2 = 0.82$). The lack of a good correlation between the computed E_a^{TS} values and the experimental ones (see above) can also account for the difference between the factor of 0.41 derived from calculations and that of 0.22 obtained[2] from experimental data. In addition, in the latter case, the value was deduced as an average value for different double bonds, in contrast to the 0.41 factor that was found using one selected monomer.

In the different $R^{\bullet}$/MA couples, the two effects can now be separated by using eqs 7, 8, and 10. In the absence of any polar effect and at $\Delta H_{r,6-31G*} = 0$, the activation energy is $E_a{}^0{}_{6-31G*} = 64.9$ kJ/mol (eq 10, $E_a{}^0{}_{6-311++G**} = 49.2$ kJ/mol). For a given system, this value is decreased from the contribution of the enthalpy ($\Delta E_{enth} = -0.41\Delta H_r$) and the polar effects (ΔE_{pol}). The enthalpy term is generally high, and the barrier depends to a large extent on the important contribution of the reaction exothermicity in the TS. The ratio $\Delta E_{pol}/(\Delta E_{enth} + \Delta E_{pol})$ helps to visualize the relative contribution of the polar effects to the decrease of the barrier height. For the $R_1^{\bullet}-R_4^{\bullet}$, $R_{11}^{\bullet}$, $R_{12}^{\bullet}$, and $R_{18}^{\bullet}$ nucleophilic radicals and the $R_{22}^{\bullet}$ electrophilic radical, the decrease of the barrier is higher than 10 kJ/mol and leads to an enhanced reactivity. Noticeable polar effects ($\Delta E_{pol} > 5$ kJ/mol) are only observed for $|\delta^{TS}| > 0.08$: such a phenomenon appears (Figure 8) for radicals characterized by a χ value lower than 3.5 eV (nucleophilic radicals) or higher than 6 eV (electrophilic radicals). This is the reason the polar effects mainly affect the E_a^{TS} vs ΔH_r correlation (Figure 4) for systems exhibiting large δ^{TS} values such as the aminoalkyl and dialkylketyl radicals.

Conclusion

The reactivity of a large variety of carbon-centered radicals toward the methyl acrylate monomer has been explored by molecular calculations. We have shown that the barrier height is strongly dependent on two important factors: the addition exothermicity and the participation of charge-transfer configurations to the transition-state structure. Despite a large influence of the enthalpy effect, the important polar effects (whose relative contributions to the barriers were clearly evaluated) are responsible for the improvement of the observed reactivity (up to a 100-fold increase for the rate constant for addition of suitable radicals to MA). Forthcoming papers will deal with the influence of the double bond on the radical reactivity and the investigation of the addition reaction of a growing polymeric radical to a monomer unit.

Acknowledgment. We are especially grateful to Pr. J.-L. Rivail for the helpful discussion on the general use of theoretical procedures and thank the CINES (Centre Informatique National de l'Enseignement Supérieur) for the generous allocation of computational time on the IBM SP3 supercomputer.

References and Notes

(1) Fouassier, J. P. *Photoinitiation Photopolymerization and Photocuring*; Hanser Publishers: Munich, New York, 1995.

(2) Fischer, H.; Radom, L. *Angew. Chem., Int. Ed.* **2001**, *40*, 1340.

(3) Fischer, H. In *Free Radicals in Biology and Environment*; Minisci, Ed.; Kluwer Academic Publishers: Dordrecht, The Netherlands, 1997.

(4) Wu, J. Q.; Beranek, I.; Fischer, H. *Helv. Chim. Acta* **1995**, *78*, 194.

(5) Arnaud, R.; Bugaud, N.; Vetere, V.; Barone, V. *J. Am. Chem. Soc.* **1998**, *120*, 5733.

(6) Shaik, S. S.; Shurki, A. *Angew. Chem., Int. Ed.* **1999**, *38*, 586.

(7) Shaik, S. S.; Canadell, E. *J. Am. Chem. Soc.* **1990**, *112*, 1446.

(8) Wong, M. W.; Pross, A.; Radom, L. *J. Am. Chem. Soc.* **1994**, *116*, 6284.

(9) Wong, M. W.; Pross, A.; Radom, L. *J. Am. Chem. Soc.* **1994**, *116*, 11938.

(10) Lalevée, J.; Allonas, X.; Genet, S; Fouassier, J. P. *J. Am. Chem. Soc.* **2003**, *125*, 9377.

(11) Lalevée, J.; Allonas, X.; Fouassier, J. P. *J. Am. Chem. Soc.* **2002**, *124*, 9613.

(12) Allonas, X.; Lalevée, J.; Fouassier, J. P. In *Photoinitiated Polymerization*; Belfield, K. D., Crivello, J., Eds.; ACS Symposium Series; American Chemical Society: Washington, DC, 2003; Chapter 12.

(13) Weber, M.; Fischer, H. H. *Helv. Chim. Acta* **1998**, *81*, 770.

(14) Knuehl, B.; Marque, S.; Fischer, H. *Helv. Chim. Acta* **2001**, *84*, 2290.

(15) Walbiner, M.; Wu, J. Q.; Fischer, H. *Helv. Chim. Acta* **1995**, *78*, 910.

(16) Beckwith, A. L. J.; Poole, J. S. *J. Am. Chem. Soc.* **2002**, *124*, 9489.

(17) Lusztyk, J.; Kanabus-Kaminska, J. M. In *CRC Handbook of Organic Photochemistry*; Scaiano, J. C., Ed.; CRC Press: Boca Raton, FL, 1989; Vol. 2.

(18) Fischer, H.; Baer, R.; Hany, R.; Verhoolen, I.; Walbiner, M. *J. Chem. Soc., Perkin Trans. 2* **1990**, 787.

(19) Colley, C. S.; Grills, D. C.; Besley, N. A.; Jockusch, S.; Matousek, P.; Parker, A. W.; Towrie, M.; Turro, N. J.; Gill, P. M. W.; George, M. W. *J. Am. Chem. Soc.* **2002**, *124*, 14952.

(20) Schnabel, W. In *Lasers in Polymer Science and Technology: Applications*; Fouassier, J. P., Rabek, J. F., Eds.; CRC Press: Boca Raton, FL, 1991; Vol. 2.

(21) Zytowski, T.; Knuehl, B.; Fischer, H. *Helv. Chim. Acta* **2000**, *83*, 658.

(22) Heberger, K.; Lopata, A. *J. Org. Chem.* **1998**, *63*, 8646.

(23) Avila, D. V.; Ingold, K. U.; Lusztyk, J.; Dolbier, W. R.; Pan, H. Q. *J. Am. Chem. Soc.* **1993**, *115*, 1577.

(24) Zytowski, T.; Fischer, H. *J. Am. Chem. Soc.* **1996**, *118*, 437.

(25) Batchelor, S. N.; Fischer, H. *J. Phys. Chem.* **1996**, *100*, 9794.

(26) Walbiner, M.; Fischer, H. *J. Phys. Chem.* **1993**, *97*, 4880.

(27) Martschke, R.; Farley, R. D.; Fischer, H. *Helv. Chim. Acta* **1997**, *80*, 1363.

(28) Heberger, K.; Lopata, A. *J. Chem. Soc., Perkin Trans. 2* **1995**, 91.

(29) Gaussian 98, Revision A.11: Frisch, M. J., Trucks, G. W., Schlegel, H. B., Scuseria, G. E., Robb, M. A., Cheeseman, J. R., Zakrzewski, V. G., Montgomery, J. A., Jr., Stratmann, R. E., Burant, J. C., Dapprich, S., Millam, J. M., Daniels, A. D., Kudin, K. N., Strain, M. C., Farkas, O., Tomasi, J., Barone, V., Cossi, M., Cammi, R., Mennucci, B., Pomelli, C., Adamo, C., Clifford, S., Ochterski, J., Petersson, G. A., Ayala, P. Y., Cui, Q., Morokuma, K., Salvador, P., Dannenberg, J. J., Malick, D. K., Rabuck, A. D., Raghavachari, K., Foresman, J. B., Cioslowski, J., Ortiz, J. V., Baboul, A. G., Stefanov, B. B., Liu, G., Liashenko, A., Piskorz, P., Komaromi, I., Gomperts, R., Martin, R. L., Fox, D. J., Keith, T., Al-Laham, M. A., Peng, C. Y., Nanayakkara, A., Challacombe, M., Gill, P. M. W., Johnson, B., Chen, W., Wong, M. W., Andres, J. L., Gonzalez, C., Head-Gordon, M., Replogle, E. S., and Pople, J. A., Gaussian, Inc., Pittsburgh, PA, 2001.

(30) Wong, M. W.; Radom, L. *J. Phys. Chem. A* **1998**, *102*, 2237.

(31) Wong, M. W.; Radom, L. *J. Phys. Chem. A* **1995**, *99*, 8582.

(32) Wong, M. W.; Pross, A.; Radom, L. *J. Am. Chem. Soc.* **1993**, *115*, 11050.

(33) Smith, D. M.; Nicolaides, A.; Golding, B.; Radom, L. *J. Am. Chem. Soc.* **1998**, *120*, 10223.

(34) Jursic, B. S. Recent Developments and Applications of Modern Density Functional Theory. *Theoretical and Computational Chemistry*; Elsevier Science: New York, 1996; Vol. 4.

(35) Skokov, S.; Whealer, R. A. *Chem. Phys. Lett.* **1997**, *271*, 251.

(36) Tsuji, T.; Ito, H.; Takeuchi, H.; Konaka, S. *J. Mol. Struct.* **1999**, *475*, 55.

(37) Nevertheless, significant differences that arise from the formation of a hydrogen bond between these radicals and the oxygen atom of the

carbonyl group in the case of the *cis* form are observed for $R_2^•$ and $R_{11}^•$: this hydrogen bond decreases the barrier by 8−9 kJ/mol for both systems.

(38) Tedder, J. M. *Angew. Chem., Int. Ed. Engl.* **1982**, *21*, 401.
(39) Arnaud, R. *New J. Chem.* **1991**, *15*, 615.
(40) Arnaud, R.; Vidal, S. *New J. Chem.* **1992**, *16*, 471.
(41) Cherkasov, A.; Jonsson, M. *J. Chem. Inf. Comput. Sci.* **1999**, *39*, 1057
(42) Burkey, T. J.; Castelhano, A. L.; Griller, D.; Lossing, F. P. *J. Am. Chem. Soc.* **1983**, *105*, 4701.
(43) Foresman, J. B., Frisch, A. In *Exploring Chemsitry with Electronic Structure Methods*, 2nd ed.; Gaussian, Inc.: Pittsburgh, PA, 1996.
(44) Parr, R. G.; Pearson R. G. *J. Am. Chem. Soc.* **1983**, *105*, 7512.
(45) Pearson, R. G. *J. Am. Chem. Soc.* **1985**, *107*, 6801.
(46) Pearson R. G. *J. Org. Chem.* **1989**, *54*, 1423.
(47) Nalewajski, R. F. *J. Am. Chem. Soc.* **1984**, *106*, 944.
(48) Pearson R. G. *J. Chem. Educ.* **1987**, *64*, 561.
(49) Stark, M. S. *J. Am. Chem. Soc.* **2000**, *122*, 4162.
(50) Stark, M. S. *J. Phys. Chem. A* **1997**, *101*, 8296.
(51) Roberts, B. P.; Steel, A. J. *J. Chem. Soc., Perkin Trans. 2* **1994**, 2155.
(52) Parr, R. G.; Szentpaly L. V.; Liu, S. *J. Am. Chem. Soc.* **1999**, *121*, 1922.